



# Helium exhaust in divertor–closure configuration with W-shaped divertor of JT-60U

A. Sakasai<sup>\*</sup>, H. Takenaga, H. Kubo, N. Akino, S. Higashijima, S. Sakurai,  
H. Tamai, K. Itami, N. Asakura

*Japan Atomic Energy Research Institute, Naka Fusion Research Establishment, 801-1 Mukoyama, Naka-machi, Naka-gun, Ibaraki-ken, 311-0193 Japan*

## Abstract

The W-shaped divertor of JT-60U was modified from inner-leg pumping to both-leg pumping. After the modification, the pumping rate was remarkably improved with both-leg pumping in a divertor–closure configuration, which means both separatrixes close to the divertor slots. In steady state, efficient helium exhaust was realized in a divertor–closure configuration with both-leg pumping in ELMy H-mode plasmas. A global particle confinement time of  $\tau_{\text{He}}^* = 0.4$  s and  $\tau_{\text{He}}^*/\tau_E = 3$  was achieved in attached plasmas, well within the range generally considered necessary for successful operation of a future fusion reactor, such as ITER-FEAT. The helium exhaust efficiency in the divertor–closure configuration was extended by 45% as compared to the one with inner-leg pumping. In the high X-point configuration with both-leg pumping, the helium exhaust efficiency and the pumping rate of deuterium deteriorated because of the backflow through the outer slot. © 2001 Elsevier Science B.V. All rights reserved.

*Keywords:* Helium exhaust; Helium beam; JT-60U; Divertor pumping

## 1. Introduction

Control of helium (He) ash is one of the key issues in future tokamak reactors, such as ITER-FEAT and SSTR (Steady State Tokamak Reactor) [1]. ITER-FEAT is designed to operate in H-modes or some other enhanced confinement regime. A detailed experimental database related to helium level regulation and He ash removal should be developed to evaluate the margin for achievement of ignition. ELMy H-mode is attractive because of its capability of steady-state operation and particle exhaust by MHD relaxation at the plasma peripheral region.

In previous helium exhaust studies on JT-60U with He beam fueling, good He exhaust capability ( $\tau_{\text{He}}^*/\tau_E = 4$ ) was successfully demonstrated in ELMy H-mode plasmas with the W-shaped divertor in steady state [2,3]. The enrichment factor of He was estimated to be about 1.0, which is five times larger than the ITER requirement of 0.2. The enrichment factor of He was defined by  $\eta_{\text{He}} = [P_{\text{He}}/2P_{\text{D2}}]_{\text{div}}/[n_{\text{He}}/n_e]_{\text{main}}$ , where

$[P_{\text{He}}/2P_{\text{D2}}]_{\text{div}}$  is the ratio of the He neutral pressure to the deuterium neutral pressure in the divertor and  $[n_{\text{He}}/n_e]_{\text{main}}$  is the ratio of the He density to the electron density in the main plasma. Helium transport in ELMy H-mode and reversed shear discharges has been investigated [3,4].

The W-shaped divertor of JT-60U was modified from inner-leg pumping to both-leg pumping in November–December, 1998. After the modification, the pumping rate and the helium exhaust efficiency were improved in a divertor–closure configuration. Helium exhaust experiment was performed to investigate the efficiency of helium exhaust with both-leg pumping in ELMy H-mode discharges. The influence of the pumping gap in a closed divertor on deuterium and helium exhaust was investigated in Alcator C-Mod [5] and ASDEX-U [6].

## 2. Modification of W-shaped divertor

The W-shaped divertor of JT-60U was modified from inner-leg pumping to both-leg pumping. In the W-shaped divertor of JT-60U, the outer exhaust slot, which has an aperture of 2 cm, was added to the existing

<sup>\*</sup> Corresponding author. Tel.: +81-29 270 7337; fax: +81-29 270 7419. E-mail address: sakasai@naka.jaeri.go.jp (A. Sakasai).

inner one (with an aperture of 3 cm) as shown in Fig. 1(a). In the case of inner-leg pumping, carbon fiber composite (CFC) tiles were used for divertor plates, top tiles of the dome and baffling tiles at the divertor throat, and graphite tiles were used for the other parts so far. Therefore, heat load to the dome bottom exceeded the limited surface temperature 600°C of the graphite tiles in the configuration of the inner/outer separatrix close to the inner/outer slots. The divertor configuration had to be kept with the gap-in and gap-out >3 cm (i.e. distances between the inner/outer separatrix and the inner/outer slots).

With the modification of the divertor pumping, all tiles of the dome were switched from graphite to CFC to prevent the problem of heat load to the dome bottom tiles. After this modification a divertor-closure configuration, which means that the gap-in and gap-out are close to 0.5–1.0 cm and the divertor throat become narrow with lower X-point configuration, could be used. The divertor experiments with both-leg pumping were started in February, 1999. The effective pumping speed for both-leg pumping was estimated to be 15.9 m<sup>3</sup>/s at about 0.1 Pa by using a gas filling method, which is 25% higher than the one for inner-leg pumping. Helium exhaust is accomplished by condensing an argon (Ar) frost layer on the liquid helium cooled surface of three NBI cryopumps for divertor pumping between successive

plasma discharges by injecting a known amount of Ar gas into the port chambers.

### 3. Experimental setup

A tangential viewing charge-exchange recombination spectroscopy (CXRS) system provides radial density profiles of fully ionized helium. CXR emission of He II 468.52 nm ( $n = 4-3$ ) is led to 0.5- and 1.0-m Czerny–Turner spectrometers through 80-m pure quartz optical fibers. The detection system for He density profile measurement consists of image-intensified double linear photodiode arrays. The calibration of the CXRS system was performed by using an integrating sphere.

A Langmuir probe array for the measurements of electron density and temperature in the divertor region and an infrared television (IRTV) camera for the heat flux measurement are used. Recycling influx profiles of deuterium are derived from the measured line intensities of D $\alpha$  with D $\alpha$  array system. The line intensity of He I (667.8 nm) in the divertor region was measured with a 60-channel optical fiber array coupled to visible spectrometers. The neutral pressure of He and D<sub>2</sub> in the divertor region linked to the exhaust ports was measured by a Penning gauge below the outer baffle. However, the Penning gauge did not work well above 0.3 Pa. The pressure in the pumping duct is one order less as compared to the pressure below the baffle. Then an ionization gauge with a range of 10<sup>-1</sup>–10<sup>-7</sup> Pa in the pumping duct was used for higher pressure measurement.

### 4. Improvement of pumping rate

Previous studies in W-shaped divertor with inner-leg pumping indicated that the private dome and inclined target type divertor were successful in preventing the upstream transport of hydrocarbons generated by chemical sputtering, thereby reducing the resultant carbon influx to the main plasma [7]. The inner-leg pumping was effective in attached divertor because of inboard-enhanced deuterium flux. On the contrary, it was not effective in detached divertor plasma because of a remarkable increase in neutral pressure near the outer strike-point with no pump. Actually, the X-point MARFE onset density was slightly reduced in the W-shaped divertor with inner-leg pumping as compared to the open divertor without pump. With the modification of the both-leg pumping, the onset density of the detachment as well as X-point MARFE gradually increases up to 15% with increasing pumping rate. The pumping rate is defined by the ratio of the deuterium particle flux exhausted with pumping to the deuterium particle flux in the divertor,  $R_{\text{pump}} = \Phi_{\text{pump}}/\Phi_{\text{div}}$ .

Fig 1(b) shows the pumping rate as a function of the gap with both-leg pumping and inner-leg pumping (gap = 3.5 cm) in ELMy H-mode plasmas at  $I_p = 1.2$  MA,  $B_t = 2.5$  T,  $P_{\text{NB}} = 12$  MW. After the modification to both-

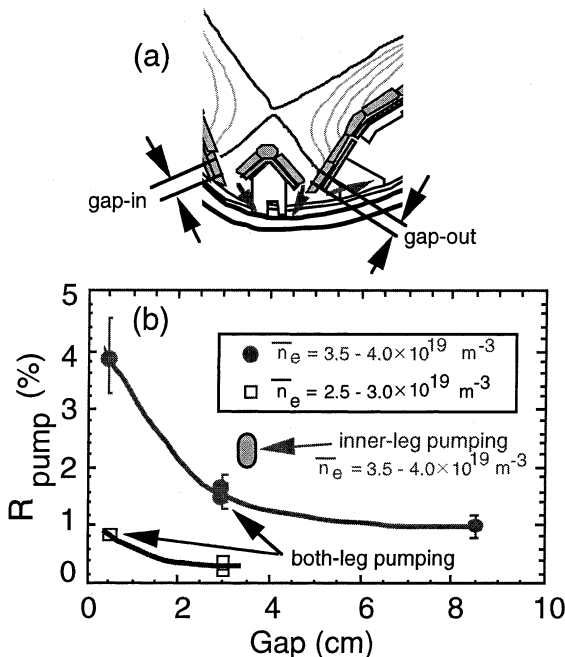


Fig. 1. (a) The W-shaped divertor of JT-60U with both-leg pumping. (b) The pumping rate as a function of the gap with both-leg pumping and inner-leg pumping (gap = 3.5 cm) in ELMy H-mode plasmas.

leg pumping, the pumping rate strongly depends on the gap-in and gap-out in L- and H-mode plasmas. Neutral particles accumulated in the inner private region are exhausted through the space under the dome. In the case of large gap-out, the back-flow to the outer divertor occurred through the outer slot and the pumping rate deteriorated. Actually, the pumping rate at the gap-in and gap-out of 3.0–3.5 cm with both-leg pumping was estimated to be about 70% of the one at the gap-in of 3.5 cm with inner-leg pumping. In order to improve the pumping rate, the divertor-closure to prevent the back-flow to the outer divertor is a key point. The pumping rate was improved up to 4% with both-leg pumping in a divertor-closure configuration at the gap-in and gap-out of 0.5 cm from 2% with inner-leg pumping at  $\bar{n}_e = 3.5\text{--}4.0 \times 10^{19} \text{ m}^{-3}$ . However, the pumping rate reduced to 1% in the lower density region at  $\bar{n}_e = 2.5\text{--}3.0 \times 10^{19} \text{ m}^{-3}$ . The pumping rate depends on the edge density, which means the particle recycling flux in the divertor. The edge density regime is  $n_{\text{edge}} = 1.5\text{--}2 \times 10^{19} \text{ m}^{-3}$  for  $\bar{n}_e = 2.5\text{--}3.5 \times 10^{19} \text{ m}^{-3}$ .

## 5. Helium exhaust in ELMy H-mode plasmas

### 5.1. Divertor-closure configuration

In the previous study, steady-state helium exhaust was successfully demonstrated in attached ELMy H-mode plasmas by using He-beam injection [3]. After the modification to both-leg pumping, helium exhaust in the divertor-closure configuration was investigated. Efficient helium exhaust was realized with He beam injection of  $P_{\text{He-NB}} = 1.4 \text{ MW}$ , which corresponds to He fueling rate of  $1.5 \times 10^{20} \text{ s}^{-1}$  (equivalent to 85 MW  $\alpha$  heating) for 3 s into ELMy H-mode discharges. Fig. 2 shows the time evolution of the electron density, the fueled D<sub>2</sub> gas puff rate, total injected NB power, He I and D $\alpha$  intensities in the divertor, He density at  $r/a = 0.68$  in an ELMy H-mode discharge ( $I_p = 1.4 \text{ MA}$ ,  $B_t = 3.5 \text{ T}$ ,  $P_{\text{NB}} = 16 \text{ MW}$ ,  $V_p = 58 \text{ m}^3$ ). Divertor-closure configuration at the gap-in and gap-out of 1 cm was kept constant for 3 s. The line-averaged electron density in the main plasma is  $\bar{n}_e = 3.8 \times 10^{19} \text{ m}^{-3}$ , which corresponds to 0.57 of Greenwald density limit  $n^{\text{Gr}}$ , and the central ion and electron temperatures at  $T_i(0) = 3.2 \text{ keV}$  and  $T_e(0) = 3.0 \text{ keV}$  in the ELMy H-mode plasma. Deuterium gas of about  $90 \text{ Pa m}^3/\text{s}$  is puffed to keep the electron density constant by a density feedback control. The position of the deuterium gas puff is the top of the main plasma. From the particle balance study, the absorbed flux by wall is estimated to be comparable to the flux with divertor pumping in the other experiments. However, the absorbed flux by wall depends on the status of wall (i.e. recycling level). The He density measured by CXRS reached a steady state at 0.9 s after the start of the He beam injection, which was  $n_{\text{He}} = 7 \times 10^{17} \text{ m}^{-3}$  ( $r/a =$

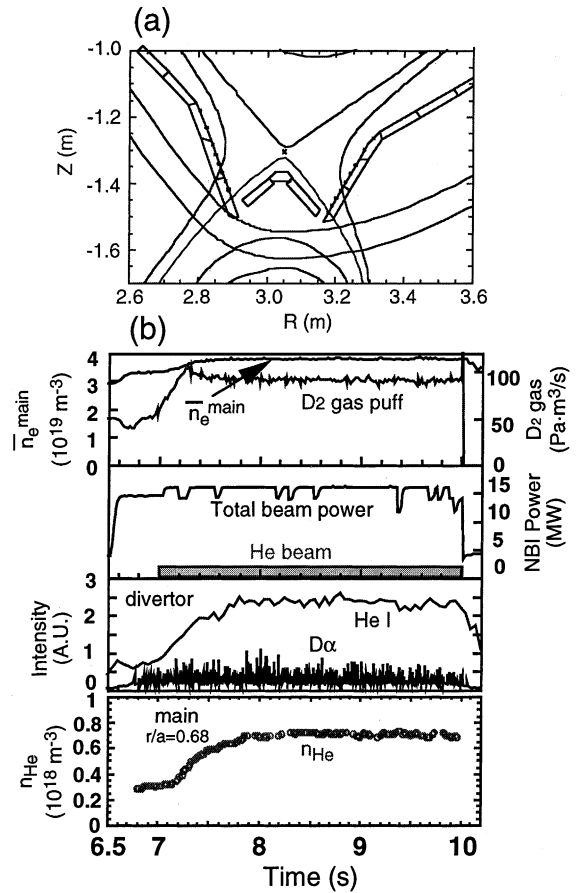


Fig. 2. (a) A divertor-closure configuration with both-leg pumping. (b) Time evolution of the electron density, the fueled D<sub>2</sub> gas puff rate, total injected NB power, He I and D $\alpha$  intensities in the divertor, helium density at  $r/a = 0.68$  in an ELMy H-mode plasma.

0.68) at  $t = 8\text{--}10 \text{ s}$ . The He concentration reached 2% of the electron density in the main plasma and was kept constant for 2 s. This indicates that the He source rate (equivalent to  $0.6 \text{ Pa m}^3 \text{ s}^{-1}$  from the He beam injection) is balanced by the exhaust rate with He pumping. The electron density in the main plasma has a broad profile and high edge density of  $\bar{n}_e = 2.5 \times 10^{19} \text{ m}^{-3}$  ( $r/a = 0.93$ ). The He density has the same profile as the electron density. In this discharge,  $\tau_{\text{He}}^* = 0.36 \text{ s}$  and  $\tau_{\text{He}}^*/\tau_E = 2.8$  with  $\tau_E = 0.13 \text{ s}$  and an H-factor ( $\equiv \tau_E/\tau_E^{\text{ITER-89P}}$ ) = 1.2 were achieved, well within the range generally considered necessary for successful operation of future fusion reactors, such as ITER-FEAT (i.e.,  $\tau_{\text{He}}^*/\tau_E = 5$ ).

### 5.2. High $X_p$ configuration

Helium exhaust efficiency was predicted to reduce in the high  $X$ -point configuration (i.e. large gap-in and gap-out) from the effect of the pumping rate on the gap. Two similar ELMy H-mode discharges with different electron

density were performed at the high  $X_p$  configuration with a gap of 4 cm. In the discharge with  $\bar{n}_e = 3.3 \times 10^{19} \text{ m}^{-3}$  ( $\bar{n}_e/n_{Gr} = 0.51$ ), the helium exhaust efficiency deteriorated to be  $\tau_{He}^* = 1.66 \text{ s}$  and  $\tau_{He}^*/\tau_E = 10$ . In the other discharge with  $\bar{n}_e = 3.7 \times 10^{19} \text{ m}^{-3}$  ( $\bar{n}_e/n_{Gr} = 0.57$ ), the helium exhaust efficiency also deteriorated to be  $\tau_{He}^* = 0.93 \text{ s}$  and  $\tau_{He}^*/\tau_E = 6.3$ . The global particle confinement time  $\tau_{He}^*$  in the high  $X_p$  configuration was double as compared to the one in the divertor–closure configuration. While, the pumping rate of deuterium in the high  $X_p$  configuration with a gap of 4 cm was estimated to be 2.2–2.8 times as compared to the divertor–closure configuration with a gap of 0.5–1.0 cm in Fig. 1(b). The dependence of helium exhaust on the gap is almost consistent with the pumping rate of deuterium.

### 5.3. Helium exhaust capability

The He exhaust capability was compared between both-leg pumping and inner-leg pumping. Fig. 3 shows the global particle confinement time  $\tau_{He}^*$  as a function of the line-averaged electron density  $\bar{n}_e$  in the main plasma. The dependence of  $\tau_{He}^*$  on  $\bar{n}_e$  in the divertor–closure configuration (gap = 0.5–1.0 cm) with both-leg pumping is almost same as the one with inner-leg pumping (gap = 3.5 cm). For example, the global particle confinement time of  $\tau_{He}^* = 0.68 \text{ s}$  in the divertor–closure configuration at  $\bar{n}_e = 3.4 \times 10^{19} \text{ m}^{-3}$  is the same as the one with inner-leg pumping. And the  $D_2$  gas puff rate of about  $40 \text{ Pa m}^3/\text{s}$  was required for both pumping configurations at this electron density. This result indicates that the He exhaust efficiency and the pumping rate of deuterium are almost same comparing both divertor configurations at the same density. However, the He exhaust efficiency was extended from  $\tau_{He}^* = 0.67 \text{ s}$  ( $P_{NB} = 13 \text{ MW}$ ) with inner-leg pumping to  $\tau_{He}^* = 0.36 \text{ s}$  ( $P_{NB} = 16 \text{ MW}$ ) with the divertor–closure configuration in the higher density region. As a result, the He exhaust

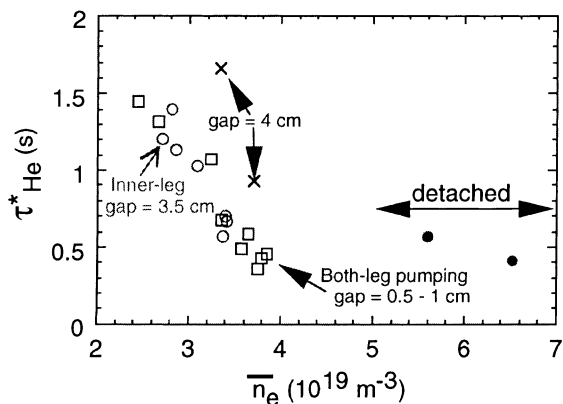


Fig. 3. The global particle confinement time  $\tau_{He}^*$  as a function of the line-averaged electron density in the main plasma.

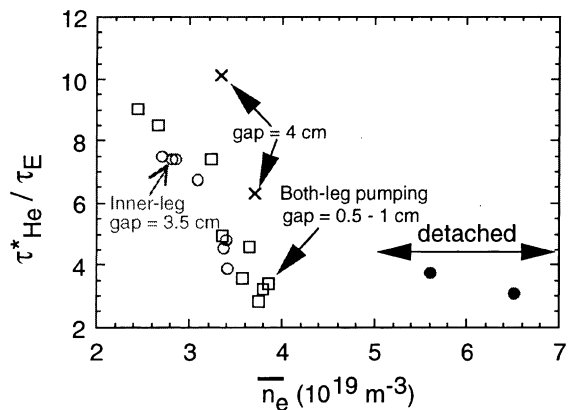


Fig. 4. The ratio of  $\tau_{He}^*/\tau_E$  as a function of the line-averaged electron density in the main plasma.

efficiency in the divertor–closure configuration was extended by 45% as compared to the one with the inner-leg pumping.

In spite of almost the same gap between inner-leg pumping (gap = 3.5 cm) and the high  $X_p$  configuration (gap = 4 cm) with both-leg pumping, the difference of the He exhaust efficiency between the two is very large. This is caused by the back-flow into the outer divertor region through the outer slot in the case of both-leg pumping. Actually, the required gas puff rate to keep the same density is smaller by 50% for the high  $X_p$  configuration with both-leg pumping.

Fig. 4 shows the ratio of  $\tau_{He}^*/\tau_E$  as a function of the line-averaged electron density  $\bar{n}_e$  in the main plasma. The dependence of  $\tau_{He}^*/\tau_E$  on  $\bar{n}_e$  in the divertor–closure configuration is also same as the one with inner-leg pumping because of the same energy confinement characteristics. However, the He exhaust capability was extended from  $\tau_{He}^*/\tau_E = 3.9$  with inner-leg pumping to  $\tau_{He}^*/\tau_E = 2.8$  with the divertor–closure configuration in the higher density region.

### 5.4. Characteristics of puff and pump

In the He exhaust experiment, gas puff and pump in the divertor–closure configuration was characterized. Fig. 5 shows (a)  $D_2$  gas puff rate required to keep the line-averaged electron density and (b) the deuterium flux in the divertor from  $D\alpha$  line as a function of the line-averaged electron density. In order to keep higher electron density than  $\bar{n}_e = 3.2 \times 10^{19} \text{ m}^{-3}$  in the divertor–closure configuration, the required gas puff steeply increases up to  $120 \text{ Pa m}^3 \text{ s}^{-1}$ , which is the maximum gas puff rate. On the contrary, the gas puff in high  $X_p$  configuration with a gap of 4 cm is reduced to 40–60% of the one in the divertor–closure configuration. The deuterium flux in the divertor increases with increasing electron density, which inclines to proportional increase

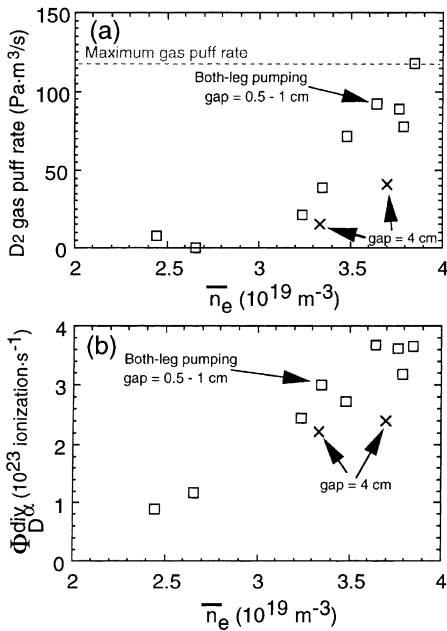


Fig. 5. (a) The D<sub>2</sub> gas puff rate required to keep the line-averaged electron density. (b) The deuterium flux in the divertor from D $\alpha$  line as a function of the line-averaged electron density.

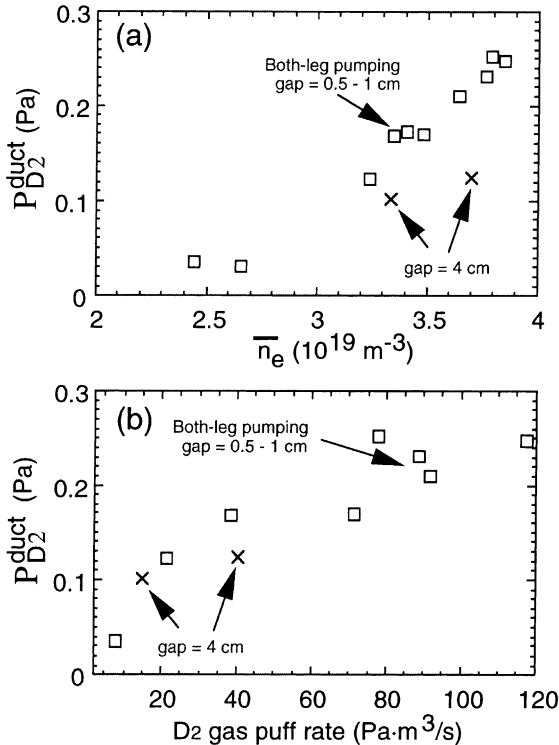


Fig. 6. The D<sub>2</sub> gas pressure in the pumping duct as function of (a) the line-averaged electron density and (b) the D<sub>2</sub> gas puff rate.

apparently in the density region. In the high  $X_p$  configuration, the deuterium flux reduces by 20–30% as compared to the divertor–closure configuration.

Fig. 6 shows the D<sub>2</sub> gas pressure in the pumping duct as a function of (a) the line-averaged electron density and (b) the D<sub>2</sub> gas puff rate. The D<sub>2</sub> gas pressure in the pumping duct increases with increasing electron density similarly to the deuterium flux in the divertor in Fig. 5(b). In the high  $X_p$  configuration, the deuterium pressure reduces by 40% as compared to the divertor–closure configuration. The D<sub>2</sub> gas pressure in the pumping duct increases with increasing D<sub>2</sub> gas puff rate.

### 6. Conclusions

The W-shaped divertor of JT-60U was modified from inner-leg pumping to both-leg pumping. After the modification, the pumping rate was improved up to 4% with both-leg pumping in a divertor–closure configuration from 2% with inner-leg pumping at the high density region. In steady state, efficient helium exhaust was realized in a divertor–closure configuration with both-leg pumping in ELMy H-mode plasmas. A global particle confinement time of  $\tau_{He}^* = 0.36$  s and  $\tau_{He}^*/\tau_E = 2.8$  was achieved in attached plasmas. As a result, the He exhaust efficiency in the divertor–closure configuration was extended by 45% as compared to the one with the inner-leg pumping.

In the high  $X_p$  configuration with both-leg pumping, the helium exhaust efficiency and the pumping rate deteriorated because of the back-flow through the outer slot. The global particle confinement time  $\tau_{He}^*$  in the high  $X_p$  configuration was double as compared to the one in the divertor–closure configuration. The dependence of helium exhaust on the gap is almost consistent with the pumping rate of deuterium.

### Acknowledgements

The authors would like to thank Drs M. Shimada, M. Kikuchi and R. Yoshino for useful discussion and advice. They would like to acknowledge the continuous support of Drs H. Kishimoto, A. Funahashi and H. Ninomiya and the contributions of JT-60 team.

### References

- [1] M. Kikuchi, Nucl. Fus. 30 (1990) 265.
- [2] A. Sakasai et al., J. Nucl. Mater. 266–269 (1999) 312.
- [3] A. Sakasai et al., IAEA Yokohama 1998, IAEA-CN-69/EX6/5.
- [4] H. Takenaga et al., Nucl. Fus. 39 (1999) 1917.
- [5] J.A. Goetz et al., J. Nucl. Mater. 266–269 (1999) 354.
- [6] H.-S. Bosch et al., J. Nucl. Mater. 266–269 (1999) 462.
- [7] N. Hosogane et al., J. Nucl. Mater. 266–269 (1999) 296.